14th Australasian Fluid Mechanics Conference
Adelaide University, Adelaide, Australia
10-14 December 2001

The Kelvin-Helmholtz to Holmboe Instability Transition in Stratified Exchange Flows

A. McC. Hogg[1] and G. N. Ivey

Centre for Water Research
University of Western Australia, Western Australia, 6009, AUSTRALIA

[1] Now At Southampton Oceanography Centre
Southampton, SO14 3ZH, UK

Abstract

A laboratory investigation of exchange flows near the two-layer hydraulic limit is used to examine the generation of shear instability at the interface dividing the two layers. Regimes characterised by either Kelvin–Helmholtz or Holmboe's instability are found to be separated by a well-defined transition. The transition from Kelvin–Helmholtz to Holmboe's instability is compared to scaling arguments that draw on elements of both two-layer hydraulic theory and linear stability theory.

Introduction

Shear instability is the process by which kinetic energy is drawn from the sheared velocity field, and converted to potential energy via mixing of a stable background density gradient. The most commonly studied class of shear instability is the Kelvin–Helmholtz (KH) instability (see [5, 6] for example). Another instability was predicted theoretically by Holmboe [4], but has rarely been observed in experiments, and has been called Holmboe's instability. In this paper we present results of laboratory experiments which enable us to examine the transition from KH to Holmboe's instability. These instabilities are observed in a bi-directional exchange flow which resembles the two-layer hydraulic solution [1] for exchange flow through a contraction.

Two layer hydraulic exchange flows

The steady state solution for density-driven exchange flow through a contracting channel is originally due to Wood [11], with further major developments from Armi [1] and Lawrence [7]. This solution is derived from the conservation of energy and mass in a two-layer, inviscid, non-diffusive fluid, and is frequently referred to as the two-layer hydraulic solution. It is sufficient for the purposes of this paper to note that, if the volume flux in each direction is equal, the difference in velocity between the two layers is constant in the streamwise (x) direction, and is given by

$$\Delta U = u_1 - u_2 = (g'H)^{1/2}, \tag{1}$$

where $u_i(x)$ is the layer velocity which is constant in z, H is fluid height and $g' = g\Delta\rho/\rho_0$ is the reduced gravity based on the density difference $\Delta\rho$ between the layers, the gravitational constant g and reference density ρ_0. Furthermore, the arithmetic mean velocity at any point is given by

$$\bar{U}(x) = \frac{u_1 + u_2}{2}, \tag{2}$$

and is always directed away from the centre of the contracting region (except at $x = 0$ where $\bar{U} = 0$).

Shear Instability

Consider a three layer background flow with piecewise profiles of fluid velocity and density as shown in figure 1. Based on Hazel [3], we define a bulk Richardson number, $J \equiv g'\delta/(\Delta U)^2$ where δ is the thickness of the shear layer. We also define a thickness of the density interface η as shown in figure 1, and the ratio of layer thicknesses $R \equiv \delta/\eta$.

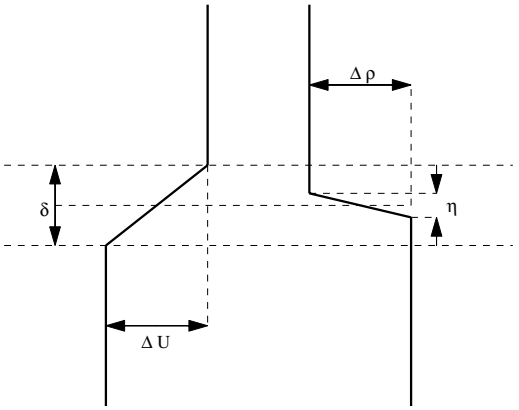

Figure 1: Piecewise profiles of velocity and density used for stability calculations.

The dominant wavelength and phase speed of instabilities in such a flow can be predicted by finding the fastest growing linear disturbance [8]. In the absence of viscosity and diffusion, the linear stability analysis for the case when $R \to \infty$ ($\eta = 0$) predicts two distinct types of instability [2]. If $J < 0.046$, an instability will form which has zero phase speed and relatively high growth rate. This is a Kelvin-Helmholtz instability [2]. For $J > 0.046$, the fastest growing instability is Holmboe's instability which has a higher wavenumber and finite phase speed relative to the mean shear. This instability is composed of a pair of oppositely propagating modes which interact to produce limited mixing of the background density gradient.

It is possible that viscosity may damp instabilities which form [9]. The extent of viscous damping will depend upon the Reynolds number, $Re \equiv \Delta U\delta/\nu$. The purpose of our experiments was to investigate the type of instabilities which formed as a function of bulk Richardson number.

Experiments

The experiments were conducted in a $2.58 \times 0.53 \times 0.60$ m tank, with a 0.50 m long perspex insert forming the contracting region. A sluice gate at the left-hand end of the insert separated fresh water in the left-hand reservoir from saline water in the right-hand reservoir. Once the sluice gate was opened, dense water flowed through the contracting channel, producing a fresh water return flow. Quasi-steady exchange flow lasted for between 3 and 9 minutes.

Measurements of the density and velocity fields were taken during the experiments. The evolution of the interface was observed by seeding fluid in the left-hand reservoir with Sodium Fluorescein, a fluorescent dye. The flow was illuminated from

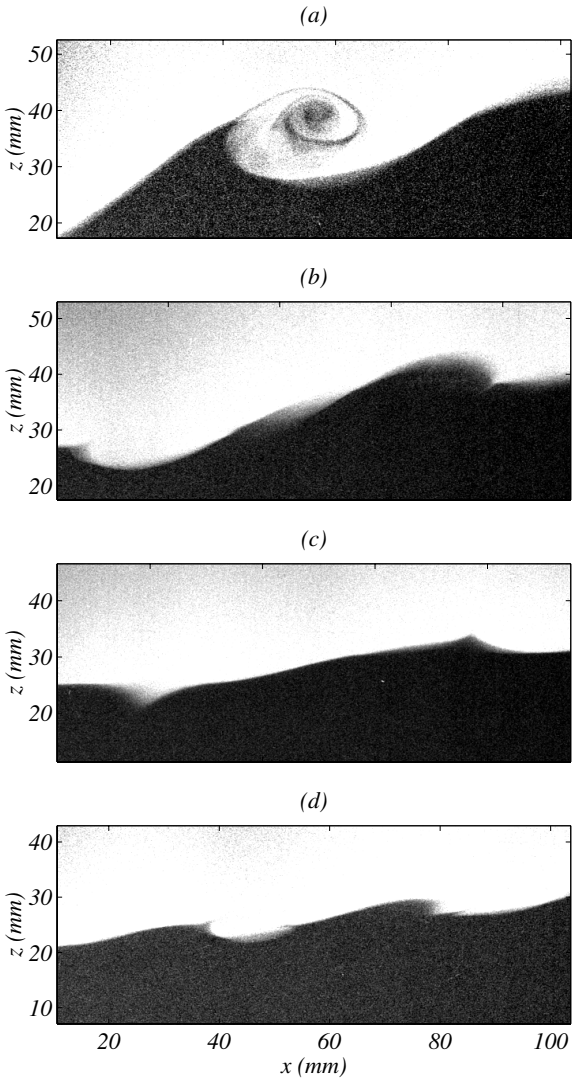

Figure 2: Still photographs from different parameter regimes. (a) Experiment S1, $J \approx 0.058$; (b) S2, $J \approx 0.084$; (c) S3, $J \approx 0.121$; (d) S4, $J \approx 0.103$.

below by a vertical light sheet of width between 5 and 15 mm. Images were taken using either a CCD video camera, or a SLR camera placed 1.6 m from the tank perpendicular to the flow. The density interface thickness η was measured by fitting a tanh function to the vertical profiles of intensity I using the definition $\eta = \Delta I/(\partial I/\partial z)_{max}$.

The velocity interface thickness was measured by dropping crystals of Potassium Permanganate of diameter 0.5–1 mm into the fluid. The crystal left a streak of dye in the fluid, allowing reconstruction of the fluid velocity profiles using images from the video camera. The interface thickness was measured from the velocity profile using $\delta = \Delta U/(\partial U/\partial z)_{max}$.

Results

When the sluice gate is opened, some mixing occurs at the boundary between the two fluids. Therefore, when the quasi-steady exchange flow forms, the interface contains some mixed fluid. The diffuse interface subsequently undergoes sharpening as a result of advection of reservoir fluid into the channel, and the divergence of the fluid as it accelerates through the contraction. In some experiments a sharp stable interface forms, which is ultimately disturbed by instabilities. In other cases the onset of instability occurs shortly after the exchange begins.

In figure 2 we show one photograph from each of four different experiments labelled S1–S4. Estimates of bulk Richardson number for each experiment is shown in the caption, and will be discussed more fully below. In experiment S1 the qualititative behaviour of KH instability is observed, as shown in figure 2(a). Large billows are formed which do not travel with respect to the mean fluid flow: the instabilities are dragged away from the centre of the contraction by the mean shear. The billows grow to large amplitude and then collapse, after which the shear flow advects fluid away from the mixed region and acts to reduce the interface thickness. Sharpening of the interface ensues, thereby decreasing stability until another perturbation forms.

Some interface perturbations in experiment S2 exhibit features of both KH and Holmboe's instability. For instance, figure 2(b) captures one such instability which overturns the central density interface, yet is travelling with respect to the mean flow. This is consistent with flows simulated by Smyth & Peltier[10] which are close to the KH–Holmboe transition point.

By decreasing the fluid height again (experiment S3, figure 2c) we reach a state which clearly shows the characteristics of Holmboe's instability. The two component Holmboe modes are shown: the downward cusping wave is travelling to the left and the upward cusping mode is travelling right.

Experiment S4 shown in figure 2(d) has the same H as S3, but double the density difference so that, according to two-layer hydraulic solution, the fluid velocities are the same as in S1. The observed flow clearly shows the character of Holmboe's instability with two oppositely propagating modes.

The evolution of instabilities with time is best visualised with space-time diagrams. To construct these diagrams we use a number of sequential video images which show the density field as indicated by the fluorescein dye. By finding interface position at all points in x and t we are able to plot the perturbation of the interface height from the running mean. This is done in figure 3 for experiments labelled I1–I4.

The transition from KH to Holmboe's instability is clearly illustrated by figure 3. A signature of KH instability is that disturbances propagate away from the centre of the contraction as shown in figure 3(a). In contrast, the Holmboe modes have constant velocity relative to the mean shear. This is shown in figure 3(c,d), with waves travelling slowly as they propagate towards the centre of the contraction, and speeding up as they exit the contraction. In figure 3(b), the x–t diagram for experiment I2, both KH and Holmboe's instability are present.

Predicting modes of instability

Scaling of stability parameters

In this section we consider some simple scaling arguments which allow us to include the first order effects of molecular viscosity and diffusion in determining the finite thicknesses η and δ in a hydraulic exchange flow and hence evaluate aspects of the stability of these flows. The finite thickness of the velocity interface, δ is due to the viscous diffusion of momentum over some timescale τ, or

$$\delta \sim (\nu\tau)^{1/2}. \tag{3}$$

The most appropriate timescale will be related to the fluid velocity and a horizontal length-scale L over which the two fluid layers are in contact, $\tau \sim L/\Delta U$. This can be combined with (1)

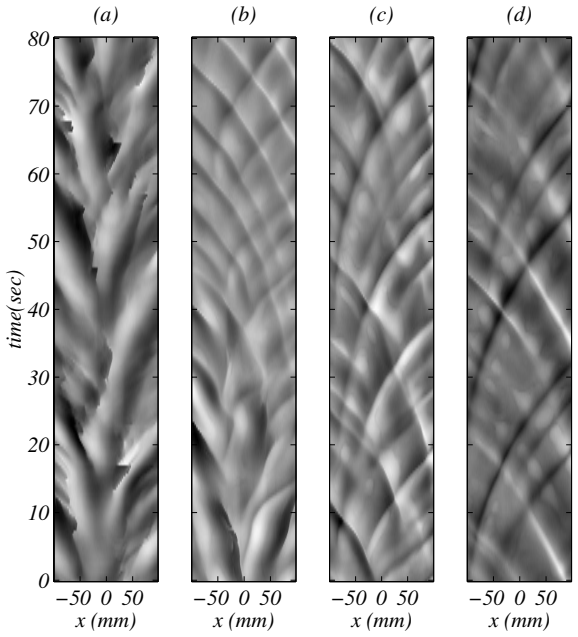

Figure 3: The evolution of instabilities shown in x–t diagrams. (a) Experiment I1, $J \approx 0.065$; (b) I2, $J \approx 0.079$; (b) I3, $J \approx 0.096$; (b) I4, $J \approx 0.119$;

and (3) to give,

$$\delta \sim \frac{(\nu L)^{1/2}}{(g'H)^{1/4}}, \tag{4}$$

which gives the dependence of the velocity interface thickness upon external parameters.

The density interface thickness can be estimated using the same technique, using the molecular diffusion of salt κ instead of ν,

$$\eta \sim (\kappa\tau)^{1/2}. \tag{5}$$

The application of this argument is complicated by the density interface being thinner than the velocity interface. Therefore, the fluid velocity at the edge of the density interface will be reduced in proportion to the ratio R of the two thicknesses. For this reason, the timescale used for estimating the density interface is $\tau \sim L/\Delta U(\eta/\delta)$, giving

$$\eta \sim \frac{\kappa^{1/3}\nu^{1/6}L^{1/2}}{(g'H)^{1/4}}. \tag{6}$$

The interface thickness is dependent on the choice of horizontal length-scale L. The dominant horizontal length-scale in the problem is the length of the channel which is the same value for both velocity and density interfaces, giving the value of the ratio of thicknesses from (4) and (6) to be

$$R \sim \left(\frac{\nu}{\kappa}\right)^{1/3} = Sc^{1/3}, \tag{7}$$

where Sc is the Schmidt number.

We are now able to estimate the bulk Richardson number in this flow. From (1), (4) and the definition of J, we obtain

$$J \sim \frac{(\nu L)^{1/2}}{g'^{1/4}H^{5/4}}. \tag{8}$$

We are also able to estimate the Reynolds number using (1), (4) and the definition of Re which gives

$$Re \sim \frac{(g'H)^{1/4}L^{1/2}}{\nu^{1/2}}. \tag{9}$$

The scaling arguments shown here demonstrate the dependence of stability parameters upon relevant external controllable parameters for the exchange flows considered here. By varying g' and H, both Re and J change, but R is constant. Note, however, that δ and Re depend weakly upon both external parameters, while J varies strongly with H. Therefore we expect H to be the primary cause of variations in stability. At large values of H, J will decrease, and KH billows are likely; as H is decreased we may pass through the transition to Holmboe's instability.

Comparison of experiments with scaling arguments

Measurements of δ and η are found to be consistent with (4) and (6) above. A close fit with experimental data is obtained by writing

$$\delta \approx 1.5\frac{(\nu L)^{1/2}}{(g'H)^{1/4}}, \tag{10}$$

and

$$\eta \approx 1.1\frac{\kappa^{1/3}\nu^{1/6}L^{1/2}}{(g'H)^{1/4}}. \tag{11}$$

The ratio of thicknesses can be calculated from (10) and (11) to give

$$R \approx 1.4Sc^{1/3} \approx 12. \tag{12}$$

This is much larger than the threshold value for the formation of Holmboe's instability, validating the use of $R \to \infty$ in the stability calculation.

Using (10) and (8) we can write

$$J \approx 1.5\frac{(\nu L)^{1/2}}{(g'H^5)^{1/4}}. \tag{13}$$

The functional dependence of J on g' and H is shown by contours of constant J in figure 4. The right-hand solid contour ($J = 0.046$) is the point at which the KH–Holmboe transition occurs in the linear theory. The left-hand solid contour ($J = 0.071$) is the point above which KH instability cannot occur in the linear theory. Figure 4 contains information about the type of instability observed in each experiment showing Holmboe's instability occurring at high J and KH instability at low J. The transition point occurs at $J \approx 0.08$.

Finally we use (9) to predict the variation of Reynolds number in the flow. Again we substitute (10) to give

$$Re \approx 1.5\frac{L^{1/2}(g'H)^{1/4}}{\nu^{1/2}}. \tag{14}$$

Note that there is a weak dependence of Reynolds number on experimental parameters, so that the range of Reynolds numbers is quite small. Nonetheless, the value of Reynolds numbers in the flow range between 160 and 220, indicating that viscosity may play a role in determining stability characteristics of the flow.

The effect of finite viscosity is to damp the high wavenumber instabilities. Smyth *et al.* [9] included viscosity in the stability

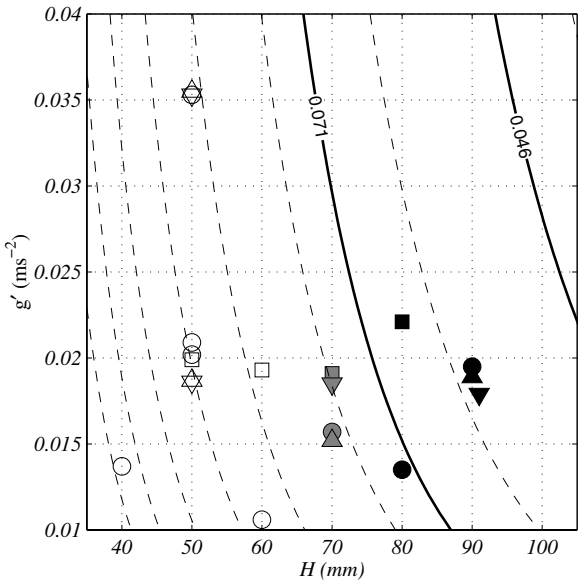

Figure 4: The value of g' versus H for each experiment. Dashed contours are levels of constant J, with the two solid contours at $J = 0.071$ and $J = 0.046$. The open symbols indicate Holmboe's instability was observed, and symbols filled with black indicate KH instability. For experiments in which both forms of instability were observed the symbol is filled grey. Experiments I are represented by the symbol □, with I1 being the filled square. Experiments S are shown by △ with S1 filled. Experiments I4 and S4 are coincident and lie in the top left quarter of the frame.

analysis and demonstrated that while the general features of the stability diagram are unchanged, viscosity may act to preferentially dampen the Holmboe modes (see figure 2 of that paper). The small Reynolds numbers in the experiments presented here indicate that it is likely that the disparity between linear stability predictions and observations of the KH–Holmboe transition is due to viscous effects.

Conclusion

Observations of the KH–Holmboe transition showed a strong dependence on the height of the exchange flow. This feature is at first startling, but can be reconciled by scaling arguments which predict the bulk Richardson number by combining two-layer hydraulic theory, one dimensional vertical diffusion and linear stability theory. The bulk Richardson number (which governs linear stability) is strongly dependent on H, the fluid height, as shown in (13), and depends weakly upon reduced gravity. This scaling was used to determine a critical value for the KH–Holmboe transition, which was found to be significantly larger than the linear stability prediction of the transition point. The disparity between the predicted and observed position of the KH–Holmboe transition is most likely due to viscosity.

Acknowledgements

We are grateful to Kraig Winters and Michael Barry for their assistance. The first author was supported by an Australian Postgraduate Award and Jean Rogerson Postgraduate Supplementary Scholarship for the duration of this work. The experimental program was supported by the Australian Research Council.

References

[1] Armi, L., The hydraulics of two flowing layers with different densities. *J. Fluid Mech.*, **163**, 1986, 27–58.

[2] Haigh, S. P., and Lawrence, G. A., Symmetric and non-symmetric Holmboe instabilities in an inviscid flow. *Phys. Fluids*, **11**, 1999, 1459–1468.

[3] Hazel, P., Numerical studies of the stability of inviscid stratified shear flows. *J. Fluid Mech.*, **51**, 1972, 39–61.

[4] Holmboe, J., On the behaviour of symmetric waves in stratified shear layers. *Geofys. Publ.*, **24**, 2, 1962, 67–113.

[5] Klaassen, G. P., and Peltier, W. R., The onset of turbulence in finite-amplitude Kelvin-Helmholtz billows. *J. Fluid Mech.*, **155**, 1985, 1–35.

[6] Koop, C. G., and Browand, F. K., Instability and turbulence in a stratified fluid with shear. *J. Fluid Mech.*, **93**, 1979, 135–139.

[7] Lawrence, G. A., On the hydraulics of Boussinesq and non-Boussinesq two-layer flows. *J. Fluid Mech.*, **215**, 1990, 457–480.

[8] Lawrence, G. A., Browand, F. K., and Redekopp, L. G., The stability of a sheared density interface. *Phys. Fluids*, **3**, 1991, 2360–2370.

[9] Smyth, W. D., Klaassen, G. P., and Peltier, W. R., Finite amplitude Holmboe waves. *Geophys. Astrophys. Fluid Dyn.*, **43**, 1988, 181–222.

[10] Smyth, W. D., and Peltier, W. R., Instability and transition in finite-amplitude Kelvin-Helmholtz and Holmboe waves. *J. Fluid Mech.*, **228**, 1991, 387–415.

[11] Wood, I. R., A lock exchange flow. *J. Fluid Mech.*, **42**, 1970, 671–687.